

# TWO EFFECTIVE AND COMPUTATIONALLY EFFICIENT PURE-PIXEL BASED ALGORITHMS FOR HYPERSPECTRAL ENDMEMBER EXTRACTION

ArulMurugan Ambikapathi, Tsung-Han Chan, Chong-Yung Chi, and Kannan Keizer

Inst. Commun. Eng., National Tsing Hua Univ., Hsinchu, Taiwan 30013.

E-mail: aareul@ieee.org, {tsunghan@mx, cychi@ee}.nthu.edu.tw

## ABSTRACT

Endmember extraction is of prime importance in the process of hyperspectral unmixing so as to study the mineral composition of a landscape from its hyperspectral observations. Though, a whole bunch of pure-pixel based endmember extraction algorithms exists, the quest for a reliable, repeatable, and computationally efficient endmember extraction algorithm still prevails. In this work, we propose two pure-pixel based endmember extraction algorithms called simplex estimation by projection (SIMPLE-Pro) algorithm and  $p$ -norm based pure pixel identification (TRI-P) algorithm. The endmember identifiability of the proposed two algorithms is theoretically proved under the pure pixel assumption. Both algorithms never require any initializations and hence they are repeatable. Monte Carlo simulations are performed to demonstrate the superior efficacy and computational efficiency of the proposed two algorithms over some existing benchmark endmember extraction algorithms.

**Index Terms**— Hyperspectral images, Endmember extraction, Pure pixels, Endmember identifiability

## 1. INTRODUCTION

Hyperspectral unmixing (HU) is a process of extracting endmember signatures and their corresponding abundance maps from the measured hyperspectral images, over a scene of interest [1]. Existing HU algorithms can basically be classified into two groups, one focusing on pure pixels (pixels in the observed hyperspectral data, that are contributed by a single endmember only) and the other without relying on pure pixels. Based on the linear mixing model (to be discussed later), identifying those pure pixels in the data cloud will directly yield the endmember signatures. Thus, the pure-pixel based algorithms aim to find the pure pixels in the given observations, and thus can only estimate the endmember signatures. Hence, those algorithms are aptly called as endmember extraction (EE) algorithms, and they are the ones considered in this work. EE algorithms currently available in the literature, include pixel purity index (PPI) [2], N-finder (N-FINDR) [3], convex cone analysis (CCA) [4], simplex growing algorithm (SGA) [5] [6], vertex component analysis (VCA) [7], and alternating volume maximization (AVMAX) [8], to name a few. Once the pure pixels (endmember signatures) are identified by EE algorithms, the corresponding abundance estimates can be obtained by using the fully constrained least squares (FCLS) algorithm [9].

Some issues associated with the above mentioned algorithms are discussed next. Firstly, for noisy observations, EE algorithms such as PPI, N-FINDR, and VCA are sensitive to initialization and hence

This work was supported by the National Science Council (R.O.C.) under Grants NSC 99-2221-E-007-003-MY3 and NSC 96-2628-E-007-003-MY3.

are not repeatable [5]. Secondly, though the computational complexity of EE algorithms is generally lower when compared to that of HU algorithms without relying on the pure pixels, it increases with the number of pixels and the number of endmembers present in the given hyperspectral data. Hence, a computationally efficient EE algorithm will always be preferred for real-time analysis of hyperspectral data. More importantly, rigorous theoretical proofs for the endmember identifiability of the above mentioned algorithms (except for AVMAX) are yet to be investigated.

The prime focus of this work is to propose reliable, repeatable and computationally efficient pure-pixel based algorithms for endmember extraction, along with a theoretical guarantee for their endmember identifiability. In this regard, we propose two endmember extraction algorithms, namely simplex estimation by projection (SIMPLE-Pro) and  $p$ -norm based pure pixel identification (TRI-P, abbreviated for Triple-P). As in the aforementioned EE algorithms, we begin with the linear mixing model for HU [2–8]. In our first algorithm (SIMPLE-Pro), the principle is to project the data onto a vector orthogonal to the affine hull of already found endmember signatures. The index corresponding to the minimum of the projected values yields a new pure pixel. In the second algorithm (TRI-P), the data are projected onto a subspace orthogonal to already found endmember signatures, and maximum  $p$ -norm is used to identify a new pure pixel. In both algorithms, prior to endmember extraction, the affine set fitting procedure [10] is used for dimension reduction, and then maximum  $p$ -norm is used to find the first endmember signature.

The notations used in this paper are briefed as follows:  $\mathbb{R}^M$  and  $\mathbb{R}^{M \times N}$  represent the set of real  $M \times 1$  vectors and  $M \times N$  matrices, respectively,  $\mathbf{1}_N$  represents the  $N \times 1$  all-one vector, and  $\mathbf{I}_N$  is the  $N \times N$  identity matrix. The symbol  $\|\cdot\|_p$  represents the  $p$ -norm and  $\mathbf{Q}^\dagger$  stands for Moore-Penrose pseudo-inverse of matrix  $\mathbf{Q}$ .

## 2. LINEAR MIXING MODEL

Consider a scenario in which a hyperspectral sensor with  $M$  spectral bands measures solar electromagnetic radiations reflecting from  $N$  distinct substances, over a scene of interest. Due to low spatial resolution, each pixel vector of the measured hyperspectral image cube can be described by an  $M \times N$  linear mixing model [1, 3, 7]:

$$\mathbf{x}[n] = \mathbf{A}\mathbf{s}[n] = \sum_{i=1}^N s_i[n]\mathbf{a}_i, \quad \forall n = 1, \dots, L, \quad (1)$$

where  $M$  is the number of spectral bands and  $N$  is the number of endmembers present in the scene. Further,  $\mathbf{x}[n] = [x_1[n], \dots, x_M[n]]^T$  is the  $n$ th pixel vector in the hyperspectral observation,  $\mathbf{A} = [\mathbf{a}_1, \dots, \mathbf{a}_N] \in \mathbb{R}^{M \times N}$  denotes the endmember signature matrix whose  $i$ th column vector  $\mathbf{a}_i$  is the  $i$ th endmember signature (or simply endmember),  $\mathbf{s}[n] = [s_1[n], \dots, s_N[n]]^T \in$

$\mathbb{R}^N$  is the  $n$ th abundance vector comprising  $N$  fractional abundances and  $L$  is the total number of observed pixel vectors.

EE algorithms aim to estimate the endmember signature matrix  $\mathbf{A}$  from the observed hyperspectral pixel vectors (or simply pixels)  $\mathbf{x}[1], \dots, \mathbf{x}[L]$ , assuming that  $N$  is known *a priori*. The following are the general assumptions in HU:

- (A1) (Non-negativity condition)  $s_i[n] \geq 0 \forall i, n$ .
- (A2) (Full additivity condition)  $\sum_{i=1}^N s_i[n] = 1 \forall n$ .
- (A3)  $\min\{L, M\} \geq N$  and  $\mathbf{A}$  is of full column rank.
- (A4) (Pure pixel assumption) There exists an index set  $\{l_1, l_2, \dots, l_N\}$ , such that  $\mathbf{x}[l_i] = \mathbf{a}_i$ , for  $i = 1, \dots, N$ .

### 3. DIMENSION REDUCTION

Like many other HU algorithms [1], we begin with dimension reduction of the observed pixels. The affine set fitting procedure in [10] is utilized for dimension reduction. The dimension-reduced pixel vectors  $\tilde{\mathbf{x}}[n]$  are obtained by the following affine transformation of  $\mathbf{x}[n]$ :

$$\tilde{\mathbf{x}}[n] = \mathbf{C}^T(\mathbf{x}[n] - \mathbf{d}) \in \mathbb{R}^{N-1}, \quad (2)$$

where  $(\mathbf{C}, \mathbf{d})$  is the affine set fitting solution given by

$$\mathbf{d} = \frac{1}{L} \sum_{n=1}^L \mathbf{x}[n], \quad (3)$$

$$\mathbf{C} = [\mathbf{q}_1(\mathbf{U}\mathbf{U}^T), \mathbf{q}_2(\mathbf{U}\mathbf{U}^T), \dots, \mathbf{q}_{N-1}(\mathbf{U}\mathbf{U}^T)], \quad (4)$$

in which  $\mathbf{U} = [\mathbf{x}[1] - \mathbf{d}, \dots, \mathbf{x}[L] - \mathbf{d}] \in \mathbb{R}^{M \times L}$ , and  $\mathbf{q}_i(\mathbf{U}\mathbf{U}^T)$  denotes the unit-norm eigenvector associated with the  $i$ th principal eigenvalue of the matrix  $\mathbf{U}\mathbf{U}^T$ . Further, due to (A2), and by substituting the signal model (1) into (2), we have

$$\tilde{\mathbf{x}}[n] = \sum_{j=1}^N s_j[n] \alpha_j, \quad (5)$$

where

$$\alpha_j = \mathbf{C}^T(\mathbf{a}_j - \mathbf{d}) \in \mathbb{R}^{N-1} \quad (6)$$

is the  $j$ th dimension-reduced endmember, by finding which, the corresponding  $\mathbf{a}_j$  can be obtained by  $\mathbf{a}_j = \mathbf{C}\alpha_j + \mathbf{d}, \forall j$  [10]. Also, it follows from (5) that under (A4),

$$\tilde{\mathbf{x}}[l_i] = \alpha_i, \quad \forall i, \quad (7)$$

and  $\tilde{\mathbf{x}}[n]$  lies in the simplex [11] formed by  $\alpha_1, \dots, \alpha_N$  [10].

### 4. SIMPLEX ESTIMATION BY PROJECTION

In this section, let us present the new EE algorithm, SIMPLE-Pro. We begin by considering the  $p$ -norm of the dimension-reduced data cloud  $\tilde{\mathbf{X}} = [\tilde{\mathbf{x}}[1], \dots, \tilde{\mathbf{x}}[L]]$ . By the triangle inequality, (A1), and (A2), one can infer from (5) that for all  $n$ ,

$$\|\tilde{\mathbf{x}}[n]\|_p \leq \sum_{i=1}^N s_i[n] \|\alpha_i\|_p \leq \max_{i=1, \dots, N} \{\|\alpha_i\|_p\}, \quad (8)$$

where  $p \geq 1$ . The inequality in (8) holds with equality if and only if  $n = l_i$  (a pure pixel index) for any  $i \in \arg \max_{k=1, \dots, N} \{\|\alpha_k\|_p\}$  (by (7)). Thus, a dimension-reduced endmember can be identified as stated in the following lemma:

**Lemma 1.** Under (A1)-(A4), a dimension-reduced endmember can be identified by

$$\alpha_i = \tilde{\mathbf{x}}[l_i], \quad (9)$$

for any  $l_i \in \arg \max_{n=1, \dots, L} \{\|\tilde{\mathbf{x}}[n]\|_p\}$ .

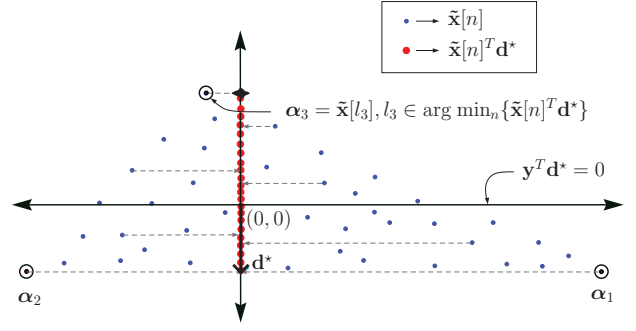


**Fig. 1.** Illustration of SIMPLE-Pro for  $N = 3$ . Assume that  $\alpha_1$  and  $\alpha_2$  have been found. The vector  $\mathbf{d}^*$  is orthogonal to the affine hull of  $\alpha_1$  and  $\alpha_2$  and the third endmember is found as  $\alpha_3 = \tilde{\mathbf{x}}[l_3]$ , where  $l_3 \in \arg \min_{n=1, \dots, L} \{\tilde{\mathbf{x}}[n]^T \mathbf{d}^*\}$ .

Now, suppose that the dimension-reduced endmembers  $\alpha_1, \dots, \alpha_k$  (where  $k < N$ ) are already identified. To find the other endmembers, we consider the following optimization problem:

$$\min_{\mathbf{d} \in \mathbb{R}^{N-1}} \|\mathbf{d}\|_2^2 \quad (10)$$

$$\text{s.t. } \mathbf{d} \in \text{aff}\{\alpha_1, \dots, \alpha_k\},$$

where  $\text{aff}\{\alpha_1, \dots, \alpha_k\}$  is the *affine hull* of  $\{\alpha_1, \dots, \alpha_k\}$ , defined as [11]

$$\text{aff}\{\alpha_1, \dots, \alpha_k\} = \left\{ \mathbf{x} = \sum_{i=1}^k \theta_i \alpha_i \mid \mathbf{1}_k^T \boldsymbol{\theta} = 1, \boldsymbol{\theta} \in \mathbb{R}^k \right\}, \quad (11)$$

in which  $\boldsymbol{\theta} = [\theta_1, \dots, \theta_k]^T$ . Note that (10) is a quadratic convex problem, and it can be easily shown that its closed-form solution is:

$$\mathbf{d}^* = (\mathbf{I} - \mathbf{B}\mathbf{B}^\dagger)\alpha_k = \mathbf{P}_\mathbf{B}^\perp \alpha_k, \quad (12)$$

where  $\mathbf{B} = [\alpha_1 - \alpha_k, \dots, \alpha_{k-1} - \alpha_k] \in \mathbb{R}^{(N-1) \times (k-1)}$  and  $\mathbf{P}_\mathbf{B}^\perp$  is the orthogonal complement projector of  $\mathbf{B}$ . By projecting all the dimension-reduced data onto  $\mathbf{d}^*$ , and by (A1) and (A2), we have

$$\tilde{\mathbf{x}}[n]^T \mathbf{d}^* = \sum_{i=1}^N s_i[n] \alpha_i^T \mathbf{d}^* \geq \min_{i=1, \dots, N} \{\alpha_i^T \mathbf{d}^*\}, \quad (13)$$

and the inequality in (13) holds with equality if and only if  $n = l_z$  for any  $z \in \arg \min_i \{\alpha_i^T \mathbf{d}^*\}$ . The  $(k+1)$ th dimension-reduced endmember can then be found as  $\alpha_{k+1} = \tilde{\mathbf{x}}[l_z]$  where

$$l_z \in \arg \min_{n=1, \dots, L} \{\tilde{\mathbf{x}}[n]^T \mathbf{d}^*\}. \quad (14)$$

The above procedure is illustrated in Figure 1, for the  $N = 3$  case. Next, in the following lemma we show that  $\tilde{\mathbf{x}}[l_z]$  is different from those endmember estimates already found.

**Lemma 2.** Suppose that  $\{\alpha_1, \dots, \alpha_k\}$  is the set of endmembers already found and  $\mathbf{d}^*$  is obtained by (12). Then, under (A1)-(A4),  $\tilde{\mathbf{x}}[l_z] \in \{\alpha_{k+1}, \dots, \alpha_N\}$  for any  $l_z \in \arg \min_{n=1, \dots, L} \{\tilde{\mathbf{x}}[n]^T \mathbf{d}^*\}$ .

*Proof:* It is well known that the projector  $\mathbf{P}_\mathbf{B}^\perp$  satisfies  $\mathbf{P}_\mathbf{B}^\perp \mathbf{B} = \mathbf{0}$ , implying

$$\mathbf{P}_\mathbf{B}^\perp (\alpha_q - \alpha_k) = \mathbf{0}, \quad q = 1, \dots, k-1. \quad (15)$$

It follows that  $\mathbf{P}_B^\perp \alpha_k = \mathbf{P}_B^\perp \alpha_q$ ,  $q = 1, \dots, k-1$ . By pre-multiplying by  $\alpha_q^T$  on both sides, we get

$$\alpha_q^T \mathbf{P}_B^\perp \alpha_k = \alpha_q^T \mathbf{P}_B^\perp \alpha_q, \quad q = 1, \dots, k-1. \quad (16)$$

Since the projector  $\mathbf{P}_B^\perp$  is positive semi-definite; i.e.,  $\alpha_q^T \mathbf{P}_B^\perp \alpha_q \geq 0$ , we have

$$\alpha_q^T \mathbf{d}^* = \alpha_q^T \mathbf{P}_B^\perp \alpha_q \geq 0, \quad q = 1, \dots, k-1. \quad (17)$$

Moreover, it is straightforward to see from (12) that  $\alpha_k^T \mathbf{d}^* \geq 0$ . Due to the nature of  $\{\tilde{\mathbf{x}}[n]\}_{n=1}^L$ , which is centered at the origin, there exists at least one vector in  $\{\tilde{\mathbf{x}}[n]\}_{n=1}^L$  such that  $\tilde{\mathbf{x}}[n]^T \mathbf{d}^* < 0$ . This can also be justified by the fact that there exists pixel vectors on either side of the hyperplane  $\{\mathbf{y} \in \mathbb{R}^{N-1} \mid \mathbf{y}^T \mathbf{d}^* = 0\}$ . Therefore (14) will never yield an index that was already identified; i.e., the new index  $l_z \notin \{l_1, \dots, l_k\}$  and further, due to (13), the obtained index must be a pure pixel index. Thus  $\tilde{\mathbf{x}}[l_z] \in \{\alpha_{k+1}, \dots, \alpha_N\}$ . ■

By repeating the above procedure for  $k = 1, \dots, N-1$ , all the dimension-reduced endmembers can be identified. The resulting EE algorithm is the SIMPLE-Pro algorithm, which is summarized in Table 1.

**Table 1.** Simplex estimation by projection (SIMPLE-Pro) algorithm.

<b>Given</b>	dimension-reduced observations $\tilde{\mathbf{x}}[n]$ , and the number of endmembers $N$ .
<b>Step 1.</b>	Find $l_1 \in \arg \max_n \{\ \tilde{\mathbf{x}}[n]\ _p\}$ . Set $\alpha_1 = \tilde{\mathbf{x}}[l_1]$ and $k = 1$ .
<b>Step 2.</b>	Define the matrix $\mathbf{B} = [\alpha_1 - \alpha_k, \dots, \alpha_{k-1} - \alpha_k]$ and find the vector $\mathbf{d}^*$ as given by (12).
<b>Step 3.</b>	Update $k := k + 1$ and then obtain $\alpha_k = \tilde{\mathbf{x}}[l_k]$ for any $l_k \in \arg \min_{n=1, \dots, L} \{\tilde{\mathbf{x}}[n]^T \mathbf{d}^*\}$ .
<b>Step 4.</b>	Go to <b>Step 2</b> until $k = N - 1$ .
<b>Step 5.</b>	Output the dimension-reduced endmember estimates $\alpha_1, \dots, \alpha_N$ .

## 5. P-NORM BASED PURE PIXEL IDENTIFICATION

In this section, we present yet another EE algorithm namely the TRI-P algorithm to find the dimension-reduced endmembers. Unlike the previous EE algorithm, here we begin by incorporating the assumption (A2) in (5) so that we have the following augmented dimension-reduced data:

$$\tilde{\mathbf{x}}[n] = \begin{bmatrix} \tilde{\mathbf{x}}[n] \\ 1 \end{bmatrix} = \sum_{i=1}^N s_i[n] \bar{\alpha}_i \in \mathbb{R}^N, \quad (18)$$

where  $\bar{\alpha}_i = [\alpha_i^T \ 1]^T$ ,  $i = 1, \dots, N$  are the augmented dimension-reduced endmembers. As in SIMPLE-Pro, following the steps leading to Lemma 1, one can show that a pure pixel index (and therefore an endmember) can be perfectly identified from  $\arg \max_{n=1, \dots, L} \{\|\tilde{\mathbf{x}}[n]\|_p\}$ , under (A1)-(A4) (see (8)).

Suppose that  $\bar{\alpha}_i$  is already found. To find a new endmember different from  $\bar{\alpha}_i$ , we consider the following subspace projection:

$$\mathbf{x}[n] = \mathbf{P}_{\bar{\alpha}_i}^\perp \tilde{\mathbf{x}}[n] = \sum_{k=1, k \neq i}^N s_k[n] \mathbf{P}_{\bar{\alpha}_i}^\perp \bar{\alpha}_k, \quad \forall n, \quad (19)$$

where  $\mathbf{P}_{\bar{\alpha}_i}^\perp = \mathbf{I}_N - \bar{\alpha}_i (\bar{\alpha}_i^T \bar{\alpha}_i)^{-1} \bar{\alpha}_i^T$  is the orthogonal complement projector of  $\bar{\alpha}_i$ . Then, a new dimension-reduced endmember can be identified as stated in the following lemma:

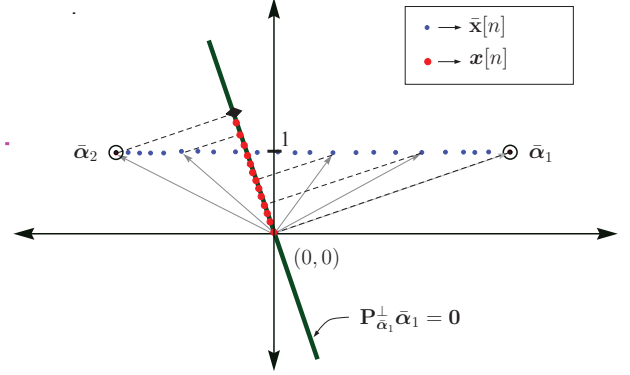


**Fig. 2.** Illustration of TRI-P for  $N = 2$ . Assume that  $\bar{\alpha}_1$  has been found.  $\bar{\alpha}_2 = \tilde{\mathbf{x}}[l_2]$ , where  $l_2 \in \arg \max_{n=1, \dots, L} \{\|\tilde{\mathbf{x}}[n]\|_p\}$ , and  $\mathbf{x}[n]$  is given by (19).

**Lemma 3.** Suppose that  $\bar{\alpha}_i$  has been found. Then, under (A1)-(A4), a new dimension-reduced endmember can be identified by

$$\alpha_j = \tilde{\mathbf{x}}[l_j] \quad (20)$$

for any  $l_j \in \arg \max_{n=1, \dots, L} \{\|\mathbf{P}_{\bar{\alpha}_i}^\perp \tilde{\mathbf{x}}[n]\|_p\}$  and  $\alpha_j \neq \alpha_i$ .

*Proof:* By the triangle inequality, (A1), (A2), and (18), we have

$$\|\mathbf{P}_{\bar{\alpha}_i}^\perp \tilde{\mathbf{x}}[n]\|_p \leq \sum_{k \neq i} s_k[n] \|\mathbf{P}_{\bar{\alpha}_i}^\perp \bar{\alpha}_k\|_p \leq \max_{k \neq i} \{\|\mathbf{P}_{\bar{\alpha}_i}^\perp \bar{\alpha}_k\|_p\}. \quad (21)$$

The inequality in (21) holds with equality if and only if  $n = l_j$  for any  $j \in \arg \max_{k \neq i} \{\|\mathbf{P}_{\bar{\alpha}_i}^\perp \bar{\alpha}_k\|_p\}$ . So one can find a new dimension-reduced endmember  $\alpha_j = \tilde{\mathbf{x}}[l_j]$  for any  $l_j \in \arg \max_{n=1, \dots, L} \{\|\mathbf{P}_{\bar{\alpha}_i}^\perp \tilde{\mathbf{x}}[n]\|_p\}$  and  $\alpha_j \neq \alpha_i$ . ■

To find the next dimension-reduced endmember, the projected data  $\mathbf{x}[n]$  is again projected onto a subspace orthogonal to the previously found endmember;  $\mathbf{P}_{\bar{\alpha}_j}^\perp \mathbf{x}[n]$ . Then by Lemma 3, one can identify another new dimension-reduced endmember. The procedure is repeated until all the  $N$  endmembers are found. The above endmember estimation methodology is the TRI-P algorithm which is summarized in Table 2. Figure 2 illustrates the idea of TRI-P for the  $N = 2$  case.

**Table 2.**  $p$ -norm based pure pixel (TRI-P) algorithm.

<b>Given</b>	dimension-reduced observations $\tilde{\mathbf{x}}[n]$ , $\tilde{\mathbf{x}}[n]$ given by (18), and no. of endmembers $N$ . Set $i = 1$ and $\mathbf{x}[n] = \tilde{\mathbf{x}}[n]$ .
<b>Step 1.</b>	Obtain $\bar{\alpha}_i = \mathbf{x}[l_i]$ for any $l_i \in \arg \max_n \{\ \tilde{\mathbf{x}}[n]\ _p\}$ .
<b>Step 2.</b>	Calculate $\mathbf{P}_{\bar{\alpha}_i}^\perp = \mathbf{I}_N - \bar{\alpha}_i (\bar{\alpha}_i^T \bar{\alpha}_i)^{-1} \bar{\alpha}_i^T$ , and update $\mathbf{x}[n] := \mathbf{P}_{\bar{\alpha}_i}^\perp \mathbf{x}[n]$ .
<b>Step 3.</b>	Update $i := i + 1$ , and go to <b>Step 1</b> if $i \leq N$ .
<b>Step 4.</b>	Output $\tilde{\mathbf{x}}[l_1], \dots, \tilde{\mathbf{x}}[l_N]$ as the estimates of $\alpha_1, \dots, \alpha_N$ .

*Remarks:* Existing pure-pixel based EE algorithms such as PPI, VCA, N-FINDR and SGA require initializations. For both of the proposed algorithms SIMPLE-Pro and TRI-P, there is no need of any initialization, and hence they are repeatable. While both TRI-P algorithm and VCA [7] involve the notion of orthogonal complement projections, there exists a subtle algorithmic difference between the two: VCA involves some sort of random vector projection in end-member estimation, but there is no randomness involved in TRI-P.

**Table 3.** Average  $\phi_{en}$  (degrees) and average computation time  $T_c$  (secs) over the various EE methods for different purity levels ( $\rho$ ) and SNRs.

Methods	$\rho$	$\phi_{en}$ (degrees)										$T_c$ (secs)
		SNR (dB)										
		0	5	10	15	20	25	30	35	40		
N-FINDR	0.6	19.61	14.95	11.13	9.14	8.41	8.42	8.57	8.53	8.60	3.61	
	0.8	19.08	14.49	10.39	8.03	6.51	6.31	5.31	5.25	5.25		
	1	19.06	14.42	10.55	8.02	<b>5.47</b>	<b>2.93</b>	1.38	0.85	0.53		
VCA	0.6	19.34	14.75	10.84	8.74	8.00	<b>7.71</b>	8.32	9.13	9.19	0.66	
	0.8	18.94	14.14	10.24	7.87	6.61	5.92	8.01	7.60	7.12		
	1	18.83	14.14	10.15	8.03	5.86	3.72	8.49	7.56	6.25		
SGA	0.6	<b>18.77</b>	<b>14.16</b>	10.68	8.69	<b>7.83</b>	7.74	7.72	<b>7.58</b>	<b>7.61</b>	0.35	
	0.8	<b>18.30</b>	13.89	10.12	<b>7.77</b>	6.72	6.09	5.62	5.49	5.37		
	1	18.40	13.93	10.20	8.02	6.09	3.37	1.24	0.75	0.41		
SIMPLE-Pro	0.6	19.09	14.27	<b>10.58</b>	8.63	7.89	7.92	7.83	7.65	7.63	0.21	
	0.8	18.49	<b>13.63</b>	10.18	7.78	6.50	6.25	5.74	5.67	5.48		
	1	<b>18.34</b>	<b>13.74</b>	<b>10.07</b>	7.99	5.93	3.63	1.32	0.79	0.47		
TRI-P ( $p = 2$ )	0.6	19.98	14.77	10.99	<b>8.45</b>	7.92	7.79	<b>7.66</b>	7.77	7.74	0.22	
	0.8	19.42	14.35	<b>10.11</b>	7.79	<b>6.41</b>	<b>5.70</b>	<b>5.14</b>	<b>4.78</b>	<b>4.54</b>		
	1	19.40	14.53	10.25	<b>7.69</b>	5.68	3.19	<b>1.13</b>	<b>0.63</b>	<b>0.36</b>		

## 6. SIMULATIONS AND CONCLUSIONS

The performance evaluation of the proposed two EE algorithms, SIMPLE-Pro and TRI-P (with  $p = 2$ ), by simulation is presented in this section. Other EE algorithms that are compared are N-FINDR, VCA, and SGA. The root-mean-square (rms) spectral angle  $\phi_{en}$  [7, 10] between the true and the estimated endmember signatures is used as the performance index. In the simulations the number of endmembers is 12 ( $N = 12$ ) and the number of observed pixels is 1000 ( $L = 1000$ ). The endmember signatures are chosen from the USGS library [12], and it has 224 bands ( $M = 224$ ). In each run, 1000 noise-free observed pixel vectors were synthetically generated following the signal model in (1), and the abundance vectors  $\mathbf{s}[n]$  were generated following Dirichlet distribution (as in [7]), for different purity levels  $\rho$  [10]. The noisy data were generated by adding independent and identically distributed zero-mean Gaussian noise to the noise-free data for different signal-to-noise ratios (SNRs), where  $\text{SNR} = \sum_{n=1}^L \|\mathbf{x}[n]\|_2^2 / ML\sigma^2$  and  $\sigma^2$  is the noise variance. For each scenario 100 independent runs are performed and the average  $\phi_{en}$  (over 100 runs) and the average computation time  $T_c$  (over all the scenarios under consideration) of each algorithm (implemented in Matlab R2008a and running in a desktop computer equipped with Dual Core CPU 2.80 GHz, 2 GB memory) are calculated, for different purity levels ( $\rho = 0.6, 0.8, 1$ ) and SNRs ranging from 0 dB to 40 dB, in steps of 5 dB.

The obtained simulation results are shown in Table 3. The bold-faced numbers in Table 3 correspond to the minimum rms spectral angle for a specific pair of ( $\rho$ , SNR), over all the algorithms under test. It can be observed from Table 3 that although the performances of all the EE algorithms are competitive, SIMPLE-Pro and TRI-P still outperform the other algorithms in most of the scenarios. On the other hand, the average computation times ( $T_c$ s) for SIMPLE-Pro and TRI-P are almost the same and they are about 17 times, 3 times and 1.5 times smaller than that of N-FINDR, VCA, and SGA, respectively. These simulation results demonstrate the efficacy and computational efficiency of the proposed two EE algorithms.

In summary, we have presented two effective and computationally efficient EE algorithms namely, SIMPLE-Pro and TRI-P and we have theoretically proved their endmember identifiability under the assumptions (A1)-(A4). It is shown via simulations that either

SIMPLE-Pro or TRI-P yields the best performance in most of the scenarios under consideration, and the computational complexities of SIMPLE-Pro and TRI-P are lower than some existing benchmark EE algorithms. The application of SIMPLE-Pro and TRI-P algorithms to real hyperspectral data is currently under investigation.

## 7. REFERENCES

- [1] N. Keshava and J. Mustard, "Spectral unmixing," *IEEE Signal Process. Mag.*, vol. 19, no. 1, pp. 44-57, Jan. 2002.
- [2] J. W. Boardman, F. A. Kruse, and R. O. Green, "Mapping target signatures via partial unmixing of AVIRIS data," in *Proc. Summ. JPL Airborne Earth Sci. Workshop*, Pasadena, CA, Dec. 9-14, 1995, pp. 23-26.
- [3] M. E. Winter, "N-findr: An algorithm for fast autonomous spectral end-member determination in hyperspectral data," in *Proc. SPIE Conf. Imaging Spectrometry*, Pasadena, CA, Oct. 1999, pp. 266-275.
- [4] A. Ifarraguerri and C.-I. Chang, "Multispectral and hyperspectral image analysis with convex cones," *IEEE Trans. Geosci. Remote Sens.*, vol. 37, no. 2, pp. 756-770, Mar. 1999.
- [5] C. I. Chang, C. C. Wu, W. M. Liu, and Y. C. Ouyang, "A new growing method for simplex-based endmember extraction algorithm," *IEEE Trans. Geosci. Remote Sens.*, vol. 44, no. 10, pp. 2804-2819, Oct. 2006.
- [6] C. I. Chang, C. C. Wu, C. S. Lo, and M. L. Chang, "Real-time simplex growing algorithms for hyperspectral endmember extraction," *IEEE Trans. Geosci. Remote Sens.*, vol. 48, no. 4, pp. 1834-1850, Apr. 2010.
- [7] J. M. P. Nascimento and J. M. B. Dias, "Vertex component analysis: A fast algorithm to unmix hyperspectral data," *IEEE Trans. Geosci. Remote Sens.*, vol. 43, no. 4, pp. 898-910, Apr. 2005.
- [8] T.-H. Chan, C.-Y. Chi, W.-K. Ma, and A. Ambikapathi, "Hyperspectral unmixing from a convex analysis and optimization perspective," in *Proc. First IEEE WHISPERS*, Grenoble, France, Aug. 26-28, 2009.
- [9] D. Heinz and C.-I. Chang, "Fully constrained least squares linear mixture analysis for material quantification in hyperspectral imagery," *IEEE Trans. Geosci. Remote Sens.*, vol. 39, no. 3, pp. 529-545, 2001.
- [10] T.-H. Chan, C.-Y. Chi, Y.-M. Huang, and W.-K. Ma, "A convex analysis based minimum-volume enclosing simplex algorithm for hyperspectral unmixing," *IEEE Trans. Signal Processing*, vol. 57, no. 11, pp. 4418-4432, Nov. 2009.
- [11] S. Boyd and L. Vandenberghe, *Convex Optimization*, UK: Cambridge Univ. Press, 2004.
- [12] Tech. Rep., Available online: <http://speclab.cr.usgs.gov/cuprite.html>.